Use of MYB as a new synthetic activator to enhance transgene expression within repressed Polycomb chromatin

Cassandra M. Barrett[1], Reilly McCracken[2], Jacob Elmer[2], and Karmella A. Haynes[1]

1. Arizona State University, School of Biological and Health Systems Engineering, 501 East Tyler Mall, Tempe, AZ 85287
2. Villanova University, Department of Chemical Engineering, 217 White Hall, 800 East Lancaster Avenue, Villanova, PA 19085

Corresponding author:
Karmella A. Haynes, karmella@asu.edu

E-mail addresses:
Cassandra M. Barrett, cmbarre6@asu.edu
Reilly McCraken, Rmccrac1@villanova.edu
Jacob Elmer, jacob.elmer@villanova.edu

ABSTRACT

Background: Epigenetic silencing of transgenes through chromatin packaging has been a persistent issue for the development of transgenic mammalian cell lines. Endogenous mechanisms are known to induce a closed chromatin state around foreign DNA before and after it has been integrated into a host cell's genome. Scientists are interested in reversing this silencing, but a lack of *a priori* knowledge of the chromatin features at transgenes hinders the rational design and application of effective strategies for transcriptional activation.

Results: Here, we systematically tested activation-associated DNA elements and proteins in transfected plasmid DNA and at epigenetically-silenced chromosomal transgenes. We demonstrated that placing DNA elements that are targeted by MYB (c-myb) and p65 upstream of a minimal promoter enhance expression from transfected plasmid DNA. To regulate the expression of chromosomally-integrated transgenes, we used proteins fused to the Gal4 DNA binding domain or dCas9/sgRNA. Three activation-associated peptides, p65, VP64, and MYB, sustained reactivation of transgene expression over 15 cell divisions in an immortalized human cell line (HEK293). Activity of the MYB fusion was inhibited by celastrol, a drug that blocks interactions between MYB and the p300/CBP histone acetyltransferase complex. Single-site targeting via dCas9-MYB was sufficient to activate transgenes within ectopic Polycomb heterochromatin and at a different site that had undergone position effect silencing.

Conclusion: Here we demonstrate the utility and flexibility of cis-regulatory elements and fusion proteins derived from natural gene regulation systems to enhance expression from epigenetically silenced transgenes. DNA motifs for p65 and MYB can be added to the transgene itself, or the activating proteins can be targeted to transgenes without enhancers to stimulate gene activation. This work has implications for determining the most appropriate strategy to enhance gene expression specifically in Polycomb-repressed chromatin.

KEY WORDS

MYB, c-myb, transgene, epigenetic silencing, activator, heterochromatin, Polycomb

BACKGROUND

The advancement of cell engineering requires robust and reliable control of endogenous and synthetic genetic material within living cells. A lack of tools for enhancing the expression of transgenes in mammalian cells currently limits effective gene regulation across contexts. The rapid formation of heterochromatin around transgenic material in mammalian cells limits our ability to express foreign DNA for the production of therapeutic proteins and the development of engineered mammalian systems for biosensing and computing [1, 2]. Integrated transgenes are often silenced by the same mechanisms that serve as a cellular defense against viral insertion into the genome [3–5]. Nucleation of heterochromatin around transgenic material can be initiated and sustained by both promoter methylation [1, 5] and various histone modifications [2, 4]. For example, MyD88 pathway-mediated silencing of transgenes leads to an accumulation of repressive H3K9me on newly bound histones [2, 6]. Silencing of transgenes may also be Polycomb-mediated, where Polycomb repressive complexes deposit H3K27me3 on histones to establish a silenced state [7–9]. The diversity and persistence of transgene silencing has led to the development of tools for mammalian cell engineering specifically aimed at combating heterochromatin.

Recruiting activators to a specific locus in order to reverse epigenetic silencing can be achieved either by including an activation-associated cis-regulatory DNA sequence within the construct itself, or through the targeting of engineered fusion proteins to the silenced transgene. Both natural and synthetic cis-regulatory motifs that recruit activators have been used [10–13] to help increase transgene expression as an alternative to viral promoters that are prone to methylation and silencing [1]. Previous screens by ourselves and other groups [11, 14, 15] have identified mammalian activation-associated cis-regulatory elements that recruit endogenous factors to increase the expression of epigenetically silenced transgenes, including motifs for nuclear factor Y, CTCF, and elongation factor alpha (EF1-□) [12, 13]. The underlying regulatory mechanisms are not entirely understood, since in this case efficient screening for functional sequences has been prioritized over dissecting the mechanism of individual elements.

Fusion proteins that target activation-associated domains to transgenes can also be used to reverse silencing. Targeted activators such as VPR, SAM, and SunTag [16–18] are composed of transcriptional activation domain (TAD) peptides, including Herpes simplex virus protein vmw65 (VP16) and nuclear factor NF-kappa-B p65 subunit (p65). Site-specific targeting of VP64 (4x VP16) has been used to increase endogenous gene expression, and remodels chromatin through the accumulation of activation-associated histone modifications (H3K27ac and H3K4me) [17, 19, 20]. Likewise, p65-based systems are very effective at restoring both endogenous [16, 21] and transgenic [22] gene expression, but have an undetermined effect on chromatin structure and accessibility.

Significant progress towards transgene reactivation has been made so far, but several important gaps remain. First, several natural mechanisms of activation are still under-investigated by biological engineers. For instance, chromatin remodelers shift, remove, or exchange nucleosomes [23], and pioneer factors increase DNA accessibility in closed chromatin by displacing linker histones [23–25]. Second, the parameters for stable transgene activation are not yet fully defined. So far, at least two studies have demonstrated prolonged enhancement of transgenes (10 to 25 days) via targeted fusion proteins alone [26] or in combination with flanking anti-repressor DNA elements [27]. Neither study evaluated the chromatin features at the target genes prior to their reactivation, therefore the context in which expression enhancement occurred is uncertain. Finally, the performance of targeted activators can be context-dependent. Catalytic domains used for site-specific chromatin remodeling [27–29], may be inhibited by pre-existing chromatin features that vary across loci. For example, Cano-Rodriguez *et al.* constructed a targeted histone methyltransferase fusion and found that the endogenous chromatin microenvironment, including DNA methylation and H3K79me, impacted the ability of their fusion to deposit H3K4me and induce activation [30]. Similarly inconsistent performance has been shown for other fusions that generate H3K79me and H3K9me [31, 32]. Systematic studies at loci with well-defined chromatin compositions are needed to fully understand mechanisms of chromatin state switching.

Here, we expand previous work where we had identified cis-regulatory sequences that enhanced expression from plasmid-borne transgenes [12]. To regulate expression of chromosomally-inserted transgenes, we compare targeted proteins that represent diverse activities: transcriptional activation through cofactor recruitment, direct histone modification, and nucleosome repositioning and displacement. We focus on reversal of silencing within Polycomb heterochromatin, which is known to accumulate at transgenes that are integrated into chromosomes [7–9] and is widely distributed across hundreds or thousands of endogenous mammalian genes that play critical roles in normal development and disease [9, 33, 34]. We report that recruitment of p65 and MYB-associated components via a cis-regulatory element or fusion proteins enhances expression from epigenetically silenced transgenes. MYB-mediated activation within Polycomb heterochromatin relies on interactions with p300 and CBP. Our results have implications for determining the most appropriate strategy to enhance gene expression, specifically within Polycomb-repressed chromatin.

RESULTS

Identification of Activation Associated Peptides

We surveyed public data to identify epigenetic enzymes and other proteins that are associated with transcriptional activation, and therefore might effectively disrupt repressive Polycomb chromatin. Polycomb-enriched chromatin typically includes Polycomb Repressive Complex 1 (PRC1: RING1A/B, PCGF1–PCGF6, CBX2, PHC1–PHC3, and SCMH1/2) [35], PRC2 (EZH1/2, EED, Suz12, and RBBP4/7) [35], H3K27me3, histone deacetylation, H2AK119ub1, and lncRNAs [35, 36]. Each activation-associated peptide (AAP) generates modifications of histone tails either by intrinsic catalytic activity or the recruitment of chromatin-modifying co-factors. In order to predict how these AAPs might influence Polycomb heterochromatin, we searched the STRING protein-protein interaction database for binding partners and their associated chromatin-modifying activities (Fig. 1).

The AAPs fall into six general categories. The transcriptional activation group, (NFkB)-p65 and the MYB (c-myb) transcriptional activation domain (TAD), includes proteins that recruit RNA Polymerase II (PolII) and p300/CBP, respectively. These AAPs have no known intrinsic gene regulation activity, and therefore rely upon the recruitment of other proteins to stimulate transcription [37–39]. We also included the recombinant TAD VP64 (four tandem copies of VP16), a popular component for synthetic activators. Histone modifications deposited by the co-activators that are recruited by these three domains are primarily associated with activation.

The histone acetylation (HAT) group includes ATF2, P300, and KAT2B. These peptides acetylate H3K27. In particular, p300 is associated with the recruitment of CBP and other co-activators that generate the activation associated mark H3K4me [40]. The histone H3 methyltransferase (H3 MT) group and the H4 methyltransferase (H4 MT) group include proteins that are either Mixed-Lineage Leukemia (MLL) complex components or SET proteins. SETD7 deposits the activation associated modification H3K4me, but its regulatory impact may vary based on local DNA methylation, which can enhance or impede co-recruitment of repressive cofactors. The histone H4 methyltransferase PRMT5 induces histone acetylation that is associated with DNA methylation in some contexts [41]. Still, PRMT5 primarily acts as an activator.

The final two groups, chromatin remodelers (CR) and pioneer factors (PF) represent activities that are relatively underexplored in the design of fusion-protein regulators. SMARCA4 is a chromatin remodeler that relies on an ATP-dependent reaction to shift the position of nucleosomes at a target site [42]. It does not mediate the deposition of histone modifications, but is associated with CBP recruitment that evicts Polycomb-associated histone modifications [43]. PFs are represented in our library by FOXA1, a winged-helix protein that displaces linker histones from

DNA to facilitate a transition to open chromatin [44]. In general, PFs bind to DNA within heterochromatin and do not catalyze histone post-translational modifications [25].

Several of the AAPs in our panel are associated with the eviction of Polycomb repressive complexes (PRCs) from endogenous genes. Accumulation of the chromatin remodeling protein SMARCA4 (BRG1) leads to the loss of PRCs at *Pou5f1* in mouse cells [45] and at *INK4b-ARF-INK4a* in human malignant rhabdoid tumor cells [46]. In the latter case, KMT2A (MLL1) also participates in PRC depletion. ATF2 interacts with a kinase that generates H3S28p, which antagonizes PRC binding [47–49]. Acetylation and methylation at H3K27 are mutually exclusive [50, 51], therefore the AAPs associated with H3K27ac (p65, MYB, ATF2, P300, KAT2B) might contribute to PRC eviction (Fig. 1). None of the AAPs in our panel are associated with enzymatic erasure of H3K27me3.

	AAP	Known Interactors								Expected Modifications in PRC Chromatin					
		HATs	HMTs	Coactivators	Kinases	Ubiquitinases	Structural	HDACs	DNMTs	H3K27ac	H3S28p	H3 / H4 Kac	H3K4me	H3R17me	H3R26me
Transcriptional activation	(NFκB)-p65	3	2	5	2			2		PE		A	A		
	VP64 (4xVP16)	1		4								A			
	MYB	2		5	1	1				PE		A			
Histone acetylation	ATF2	3		3	1					PE	PE	A			
	P300	2	2	9						PE		A	A	A	A
	KAT2B (PCAF)	8		4				1		PE		A	A		
H3 MT	KMT2A (MLL1)	2		5								A	A		
	KMT2D (MLL2)	1	9	2								A	A		
	KMT2C (MLL3)	1	7	1			1					A	A		
	KMT2E (MLL5)	1	8		2		1						A		
	SETD1A (SET1)		10			1	2						A		
	SETD1B (SET1B)		10		1		1						A		
	SETD7 (SET7/9)		2	4			2		1				A		
H4 MT	PRMT5 (ANM5)		3	2			2		1			A			
CR	SMARCA4 (BRG1)	1		12				1		PE					
PF	FOXA1 (HNF-3A)			3				1							

Figure 1. Activation-associated histone modifications associated with activation-associated peptides (AAPs) used in this study. Interaction partners determined by STRING analysis are listed in Supplemental Table S1. Previous work that characterized each AAP is cited in Supplemental Table S2. H3 MT = histone H3 methyltransferase, H4 MT = histone H4 methyltransferase, CR = chromatin remodeler, PF = pioneer factor, PE = Polycomb eviction, A = transcriptional activation.

Cis-regulatory elements recognized by transcriptional activators p65 and MYB enhance expression from an extra-chromosomal transgene

First, we used enhancer DNA elements to regulate expression from transiently-transfected plasmid DNA. Work from our group [52] and others [53, 54] has shown that plasmid DNA becomes occupied by histones, which may contribute to transgene silencing in human cells. In a previous study, we used DNA sequences that were known targets of endogenous activation-associated proteins to reduce silencing of a *luciferase* reporter gene [12]. Here, we tested additional motifs (Fig. 2a) that are recognized by AAPs from the transcriptional activator group in our panel: MYB and p65 (Fig. 1).

One of three MYB enhancer variants or the p65 enhancer was placed in either a forward or reverse orientation upstream of an EF1a promoter and a *luciferase* reporter (Fig. 2b). PC-3 (human prostate cancer) cells were transfected with each plasmid as described previously [12]. The highest levels of enhanced expression were observed for MYB variant A (4.5-fold, $p = 0.03$) or p65 (5-fold, $p = 0.08$) placed in the reverse orientation (Fig. 2c). Interestingly, switching the orientation of these motifs eliminated the enhancement effects. Nonetheless, these results suggest that cis-regulatory elements from the p65 and MYB systems can be used to attract endogenous transcriptional activators to a synthetic promoter to drive transgene expression.

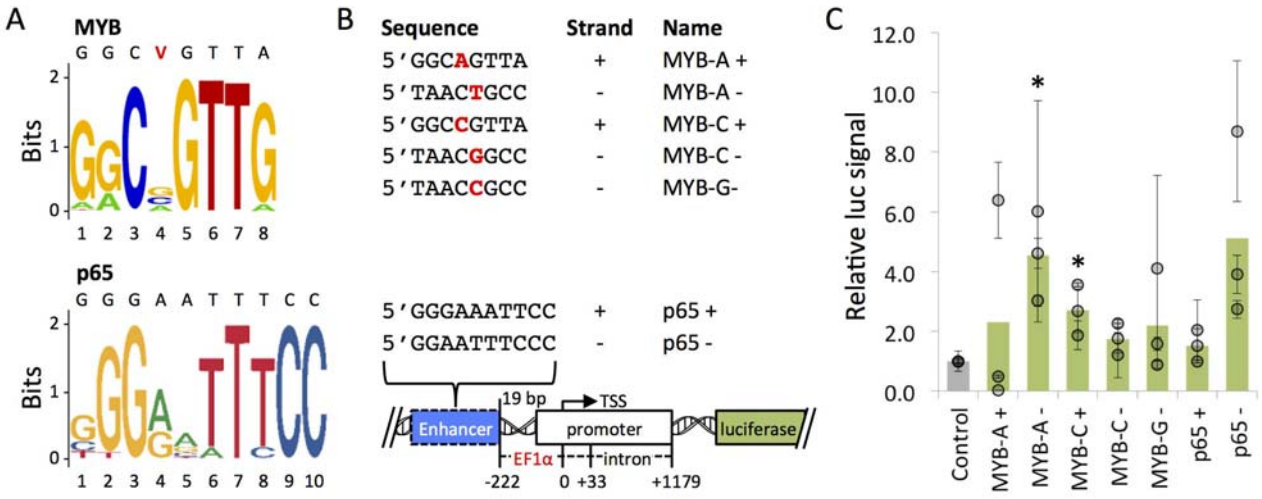

Figure 2. Luciferase expression from MYB- and p65-enhancer constructs. A) Enhancer motif logos for MYB and p65 were generated by JASPAR [55]. The MYB sequence includes a variable site (V) equally occupied by A, C, or G nucleotides. B) *Luciferase* reporter constructs (center) included one of the enhancer sequences (MYB-A +, etc.) 19 bp upstream of an EF1α promoter, or no enhancer (Control). C) Luciferase assays were carried out using PC-3 cells transfected with Lipofectamine-plasmid complexes. For each transfection, luminescence (luc signal) values were measured in triplicate and normalized to the average signal from the Control. Circle = mean normalized signal from a transfection, error bars = standard deviation. Wide bars

represent the average of three transfections. Asterisks (*) = $p < 0.05$ for the experimental average, relative to the Control average.

Identification of fusions with robust activity within Polycomb heterochromatin

Next, we asked whether the individual peptides MYB and p65, as well as other AAPs could enhance transgene expression in the absence of a specific enhancer sequence. To determine AAP activity within silenced chromatin, we targeted AAP fusion proteins (Fig. 1) to a chromosomal *luciferase* reporter that had been previously targeted by Polycomb repressive complexes (PRCs). The AAP open reading frames (ORFs) encode catalytic subunits or full length proteins (Fig. 3) that have been shown to support an epigenetically active state in various prior studies [37, 38, 42, 44, 56–62]. All of these ORFs exclude DNA binding and histone binding domains, except for the ORF encoding FOXA1 which has a catalytic domain that requires histone interactions. We cloned each ORF into mammalian vector 14 (MV14) (Fig. 3) to express a Gal4-mCherry-AAP fusion. The Gal4 DNA binding domain serves as a module to target AAPs to UAS sequences in the transgene, while the mCherry tag allows for protein visualization and quantification of the activator fusion.

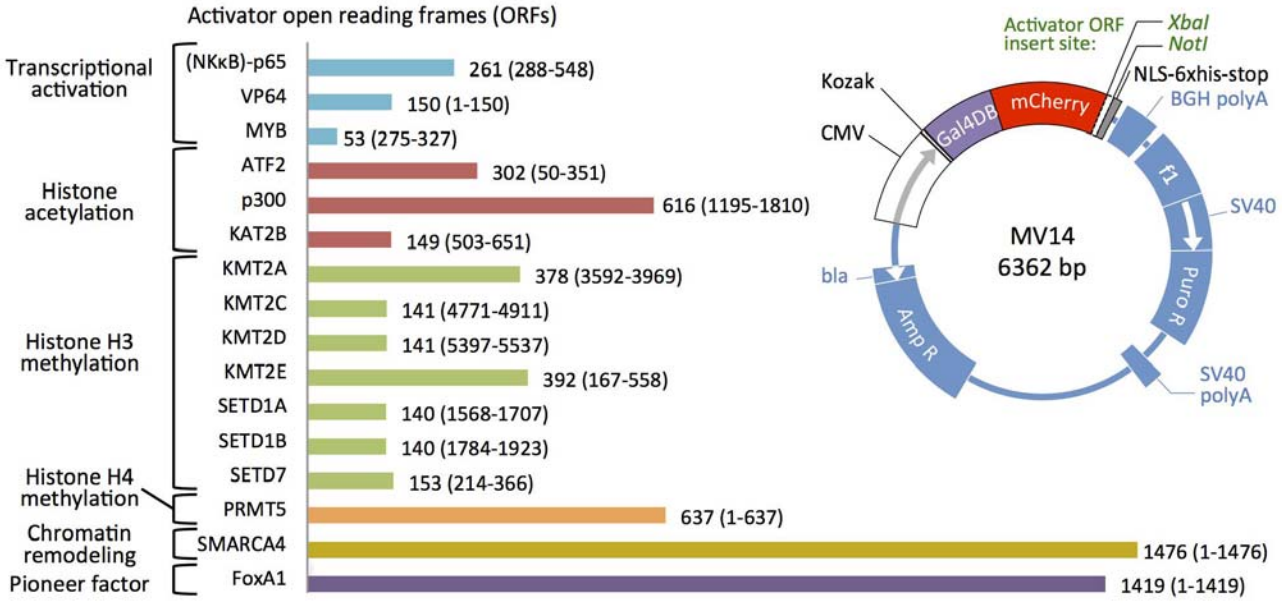

Figure 3. Design and construction of Activation-associated peptide (AAP) -Gal4 fusions. Amino acid lengths are indicated as well as domain location within the full length wild-type sequence (Supplemental Table S2). ORFs were cloned into MV14 to express a Gal4-AAP fusion protein from a cytomegalovirus (CMV) promoter. Gal4-AAPs are expressed with a C-terminal nuclear localization signal (NLS) and a 6X histidine tag. MV14 expresses puromycin resistance to enable selection of Gal4-AAP positive cells.

We tested all sixteen Gal4-AAP candidate fusion activators at repressive chromatin in HEK293 (human embryonic kidney) cells. The HEK293 cell line Gal4-EED/luc, carries a stably integrated *firefly luciferase* transgene with an upstream Gal4UAS (*Gal4UAS-Tk-luciferase*) (Fig. 4a) [22, 63]. The cells also carry a *TetO-CMV-Gal4EED* construct, which encodes a Gal4 DNA-binding domain (Gal4) fused to an embryonic ectoderm development (EED) open reading frame under the control of TetO-CMV promoter (Fig. 4a). Expression of the Gal4-EED fusion protein is controlled by a Tetracycline repressor (TetR). The addition of doxycycline (dox) to cultured Gal4-EED/luc cells releases the TetR protein from *TetO-CMV-Gal4EED*, initiating expression of Gal4-EED. Gal4-EED binds to the Gal4UAS site upstream of *luciferase*, recruiting PRC2 to the reporter. Expression of *luciferase* is switched from active to silenced through accumulation of polycomb chromatin features, which have been detected by chromatin immunoprecipitation (ChIP) experiments: EZH2, Suz12, CBX8, depletion of H3K4me [63], and gain of H3K27me3 [22, 63]. This system allows us to test the activity of Gal4-AAPs with a priori knowledge of the chromatin environment at the target gene.

Gal4-EED/luc cells were treated with dox for 48 hours to induce heterochromatin at the *luciferase* transgene. Afterwards, dox was removed and cells were grown for four days without dox to allow for Gal4-EED depletion. Cells were then transfected with individual Gal4-AAP plasmids. *Luciferase* expression was measured 72 hours post transfection.

Three of the sixteen Gal4-AAP-expressing samples showed increased luciferase levels compared to a mock-transfected control (Lipofectamine reagent only) ($p < 0.05$) (Fig. 4a). Lack of enhanced luciferase expression for the other fusions could have been due to strong inhibition by PRC complexes or failure of the AAPs to function as Gal4 fusions at the UAS site. Therefore, we also tested the activities of the fusion proteins within open chromatin. We used a parental HEK293 cell line, Luc14, that carries the *firefly luciferase* construct (*Gal4UAS-Tk-luciferase*) but lacks the *TetO-CMV-Gal4EED* repression cassette (Fig. 4b) [63]. *Luciferase* is constitutively expressed at high levels in Luc14.

We found a similar trend of expression enhancement at open chromatin in Gal4-AAP-expressing cells (Fig. 4b), where only three Gal4-AAP fusions were able to stimulate expression when positioned at the promoter-proximal UAS (Fig. 4b). In both chromatin states, AAPs from the transcriptional activation group (Fig. 1, Fig. 3) significantly increased expression compared to a mock transfection control ($p < 0.05$) by up to five fold. Our results are consistent with previous studies where p65, VP64, or MYB stimulated gene expression from a promoter-proximal site [37–39]. Here, we have demonstrated activities of these proteins within highly PRC-enriched chromatin.

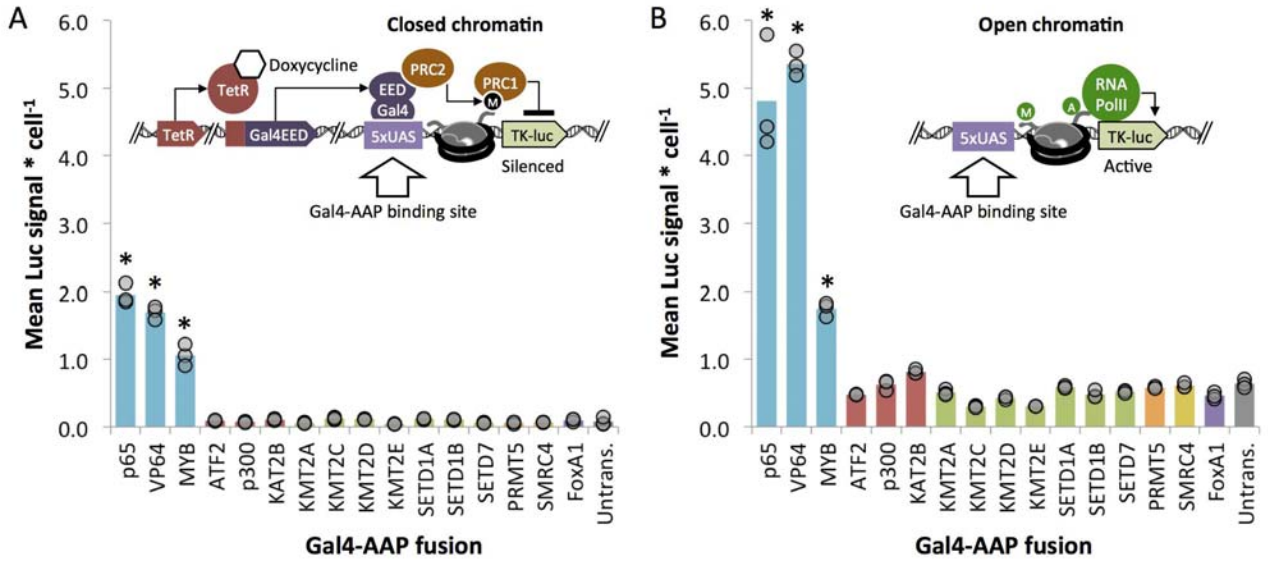

Figure 4. Measurement of *luciferase* reporter expression within closed or open chromatin after exposure to Gal4-AAP fusions. A) In Gal4-EED/luc HEK293 cells, PRC is recruited to the Tk-luciferase reporter gene via Gal4-EED (induced by dox). Treated cells were transfected with each Gal4-AAP fusion plasmid. Seventy-two hours post transfection luciferase signal was measured. Each circle in the bar graph shows the mean luciferase (Luc) signal for a single transfection, divided by cell density (total DNA, Hoechst staining signal). Bars show means of three transfections. Asterisks (*) = $p < 0.05$ compared to untransfected cells. B) The same procedure was carried out for unsilenced *Tk-luciferase* (in Luc 14 cells).

Fusion-induced activation is sustained after loss of the Gal4-AAP transactivator

The results so far were obtained at a single time point after Gal4-AAP expression. We were interested in determining whether transgene activation within polycomb chromatin is stable or is transient and susceptible to eventual re-silencing [64]. To investigate this question, we performed time-course experiments to measure expression from re-activated *luciferase* over time. We induced Polycomb heterochromatin in Gal4-EED/luc cells as described for the previous experiments. Twenty-four hours post transfection with one of the strong activators, Gal4-p65, -VP64, or -MYB, cells were grown in medium supplemented with 10 µg/mL puromycin to select for Gal4-AAP positive cells. Seventy-two hours post transfection, we measured *luciferase* expression, Gal4-AAP mRNA levels, and mCherry fluorescence from a sample of each transfected culture. The cells were then passaged in puromycin-free medium to allow for loss of Gal4-AAP, sampled every four days (approximately three generations), and the same three measurements (luciferase, Gal4-AAP mRNA, and mCherry) were repeated at each time point.

We found that transient induction by Gal4-AAPs was sufficient to induce mitotically-heritable reactivation of *Tk-luciferase* in Polycomb heterochromatin. For all three Gal4-AAP fusions, *luciferase* expression was significantly increased at most time points and at 456 hours ($p <$

0.05) compared to a mock transfection control (Lipofectamine reagent only) (Fig. 5a). In two of the three additional trails, Gal4-p65 and Gal4-MYB showed at least ~2-fold enhancement at 360 hours (Supplemental Fig. S1). Steep declines of Gal4-AAP mRNA and mCherry fluorescence after 72 hours (Fig. 5b, 5c) confirmed the transient presence of the transactivators. Therefore, enhancement of luciferase expression persisted long after depletion of each Gal4-AAP, suggesting heritable epigenetic memory of the activated state.

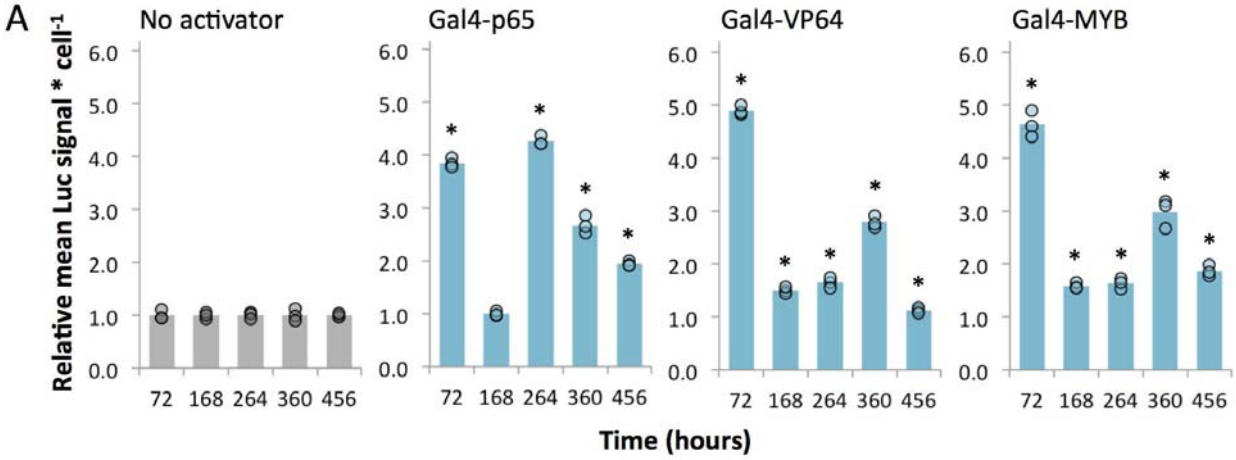

B RT-qPCR: mRNA fold change (ΔΔCq)

	72	168	264	360	465	hours
Gal4-p65	5196.5	26.2	3.9	6.3	9.1	
Gal4-VP64	7281.4	1141.5	37.3	21.5	1.4	
Gal4-MYB	3893.0	18.4	14.4	21.2	1.6	

C Flow cytometry: Median RFP signal * cell^{-1}

	72	168	264	360	456	hours
Gal4-p65	224.0	0.0	0.0	0.0	0.0	
Gal4-VP64	69.0	0.0	0.0	0.0	0.0	
Gal4-MYB	163.3	0.0	0.0	0.0	0.0	

Figure 5. Expression of Polycomb-repressed *Tk-luciferase* over time after expression and loss of Gal4-p65, Gal4-VP64 or Gal4-MYB. A) Gal4-EED/luc cells were treated with dox to induce polycomb chromatin, transfected with a Gal4-AAP plasmid, and grown under puromycin selection (10 µg/mL). At 72 hours post transfection, cells were sampled for luciferase (Luc) assays, passaged in puromycin-free medium, then sampled 168, 264, 360, and 465 hours post transfection for additional Luc assays. Mean Luc signal per cell is presented as described for Figure 4, except individual values (circles) at each time point are normalized by the mean of the "No activator" negative control. Asterisks (*) = $p < 0.05$ compared to the negative control. Results from replicate trials are shown in Supplemental Fig. S1. B) Reverse transcription followed by quantitative PCR (RT-qPCR) with primers against mCherry was used to determine Gal4-AAP transcript levels. “mRNA fold change” represents the Cq value normalized by the Cq of a housekeeping gene (*TBP*), and relative to mock-transfected “No activator” cells (Lipofectamine reagent only), log2 transformed. C) Flow cytometry of mCherry signal (red fluorescent protein, RFP) was used to determine Gal4-AAP protein levels. Data in B and C were generated from one set of transfections in A. For other samples, cells were visually inspected for RFP to verify the loss of Gal4-AAP.

MYB-mediated activation within closed chromatin requires interactions with a histone acetyltransferase

Next, we used specific chemical inhibitors to probe the mechanism of MYB-driven enhancement. The TAD core acidic domain of human MYB (D286-L309) included in our Gal4-MYB fusion construct is known to interact with a protein heterodimer of p300 and CBP (Supplemental Fig. S2). A single base pair mutation within the MYB TAD domain (M303V) disrupts p300 recruitment and subsequent activation by MYB indicating that this recruitment is crucial to activation by MYB [65, 66]. The p300/CBP histone acetylation complex deposits H3K27ac in opposition to H3K27me3 induced by PRC2 [67, 68]. Therefore, induced activation within Polycomb heterochromatin may be driven by histone acetylation.

To test this idea, we treated cells with two compounds that are known to disrupt the activity of the MYB/p300/CBP complex. Celastrol is a minimally toxic pentacyclic triterpenoid that directly inhibits the MYB/p300 interaction, by binding to the KIX-domain of CBP which serves as a docking site for the formation of the MYB/p300/CBP complex [69–72] (Fig. 6a). C646, a pyrazolone-containing small molecule, binds the p300 catalytic domain and thus directly and selectively inhibits p300 HAT activity regardless of its association with MYB (Fig. 6a) [73–75]. These compounds allow us to resolve the roles of complex assembly and p300-mediated histone acetylation during Gal4-MYB-mediated activation.

Gal4-EED/luc cells were treated with dox to induce polycomb chromatin and transfected with Gal4-MYB as described for previous experiments. We treated these cells with 5 μM celastrol or 5 μM C646 for six hours. MTT assays indicated no toxicity to HEK293 cells at this concentration (Supplemental Fig. S3). We expected luciferase assays to show a decrease in Gal4-MYB-induced expression in drug-treated cells compared to an untreated control. We observed a significant ($p < 0.05$) decrease in *luciferase* expression in celastrol-treated cells, but not in C646-treated cells (Fig. 6b). This result suggests that Gal4-MYB activity requires MYB TAD and p300/CBP assembly, while p300 HAT activity is dispensable. The other two strong activators, Gal4-VP64 and -p65, were insensitive to celastrol and C646 (Fig. 6b), indicating a p300/CBP-independent mechanism for these two fusions.

In a time-course experiment using celastrol, we observed that Gal4-MYB-mediated activation is reversible. Eighteen hours after removal of celastrol from Gal4-MYB-treated cells, *luciferase* expression levels increased ($p < 0.05$ compared to repression at t = 6), nearly restoring expression to original levels (t = 0) (Fig. 6c). Re-addition of celastrol led to a loss of Gal4-MYB induced expression (Fig. 6c).

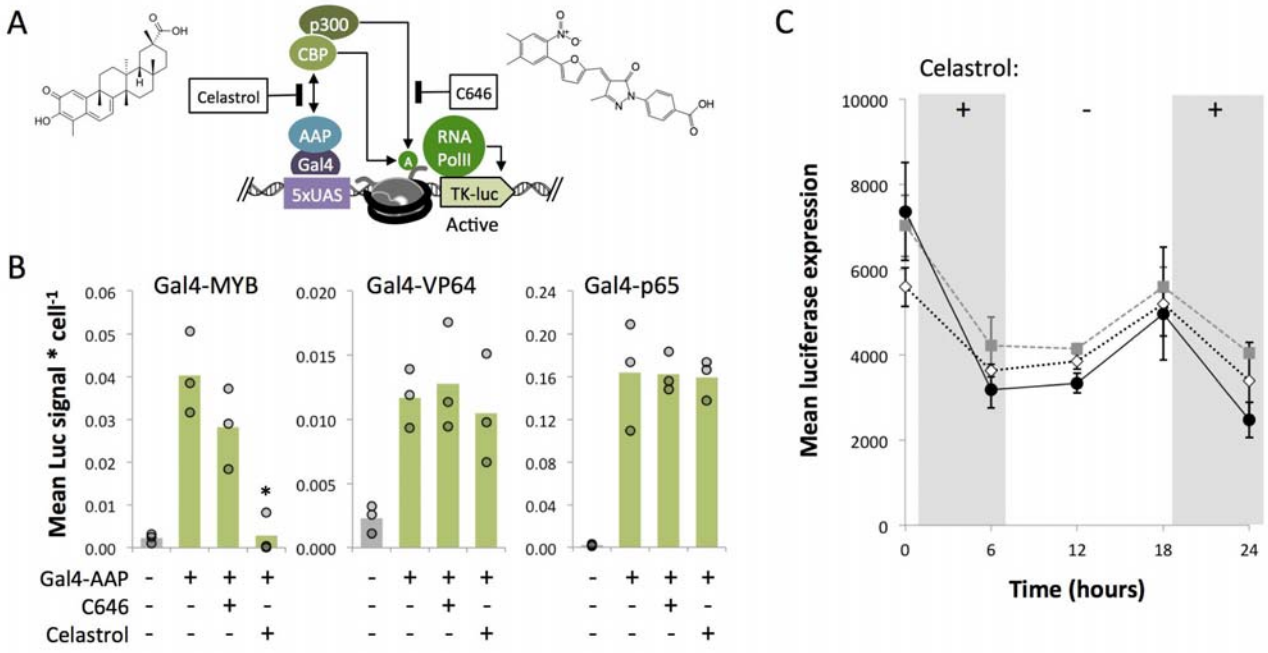

Figure 6. Celastrol disrupts Gal4-MYB-mediated activation of *luciferase* in closed chromatin. A) The p300/CBP complex acetylates histones via the catalytic HAT domain of p300 and/or CBP [68]. Celastrol inhibits the recruitment of p300/CBP by MYB by binding a docking domain in CBP that facilities complex assembly [70, 72]. C646 disrupts histone acetylation by binding the active site of p300 [75]. B) Seventy-two hours after Gal4-EED-mediated repression of *Tk-luciferase* and transfection with Gal4-AAPs, cells were treated with either 5 μM celastrol or 5 μM C646 for six hours and collected for luciferase assays. Mean luciferase (Luc) signal per cell is presented as described for Figure 4. Asterisks (*) = $p < 0.05$ compared to Gal4-MYB without drug treatment. C) Luc measurements were carried out in Gal4-MYB-expressing cells after removal (-) and re-addition (+) of celastrol. Each series represents an independent transfection. Point = mean of three luciferase assays, bars = standard error.

MYB-mediated activation in Polycomb heterochromatin relies upon proximity to the transcriptional start site

Next we asked whether MYB-mediated activation at transgenes is context dependent. We leveraged the flexible dCas9/sgRNA system to target the MYB TAD to several sites along the *luciferase* transgene (Fig. 7a). To do so, we targeted sites at different positions within the *Tk-luciferase* gene. We also tested the MYB TAD at a different transgene, *CMV-GFP* in HEK293, that had become silenced after several passages (C. Liu, unpublished).

We induced Polycomb heterochromatin in HEK 293 Gal4EED/luc cells with dox, followed by washout of dox to allow Gal4-EED depletion as described above. We transfected the cells with one of four dCas9-MYB constructs, each carrying a different sgRNA targeted at the *luciferase*

transgene. After 72 hours, we tested *luciferase* expression and found that dCas9-MYB targeted nearest the transcription start site (+9) was able to restore levels of expression similarly to Gal4-MYB (Fig. 7b). In induced Polycomb heterochromatin we observed clear position effects, as the downstream target sites show levels of activation significantly lower than Gal4-MYB ($p < 0.05$).

After determining the viability of dCas9-MYB to act as an activator for silenced transgenes in a defined chromatin environment, we wanted to test this domain against endogenous heterochromatin at the *CMV-GFP* transgene. The construct, *GFP* under the control of a CMV promoter, was inserted via Cas9-mediated HDR into a non-protein-coding region of the HEK293 genome (HEK293 site 3 [76]). We transiently transfected the cells with dCas9-MYB constructs, each carrying one of four different sgRNAs targeted upstream, within the promoter, or in the coding region of the transgene. Seventy-two hours post transfection, we used flow cytometry to measure GFP fluorescence compared to a mock-transfected control (Lipofectamine reagent only). We found that GFP fluorescence was significantly higher ($p < 0.05$) in all dCas9-MYB-expressing cells regardless of gRNA position (Fig. 7c), indicating that MYB-mediated activation does not require proximity to the TSS in all contexts.

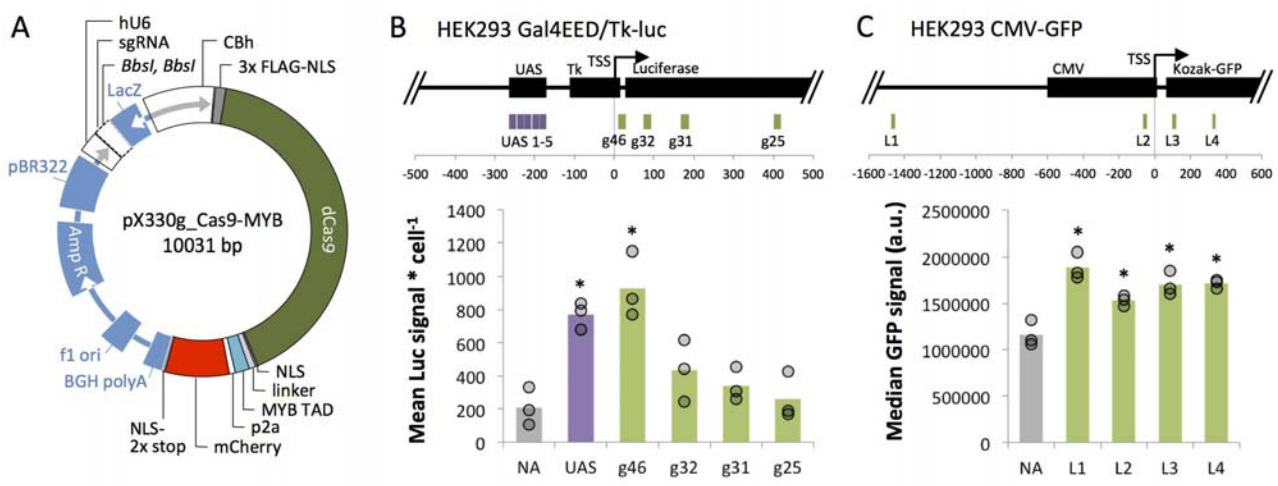

Figure 7. dCas9-MYB's ability to enhance expression in induced Polycomb heterochromatin is dependent upon distance from the promoter. A) Expression vector pX330g_dCas9-MYB was constructed from vector pX330A_dCas9 (a gift from Takashi Yamamoto, Addgene plasmid #63598) to co-express a dCas9-MYB fusion protein and mCherry from a CBh promoter. Single-stranded guide RNA sequences (Supplemental Table S3) were cloned into the BbsI sites and expressed from a hU6 promoter on the same vector. B) We targeted dCas9-MYB to four locations (g46, g32, g31, g25) across the *Tk-luciferase* transgene in silenced Gal4-EED/luc cells. Mean luciferase signal per cell is presented as described for Figure 4. The control (grey bar) is a mock-transfection with Lipofectamine (No Activator, NA). C) We targeted dCas9-MYB to four sites (L1-4) across a chromosomal *CMV-GFP* transgene in HEK293 cells. Seventy-two hours post transfection with dCas9-MYB/sgRNA vectors or mock transfection, we measured GFP fluorescence via flow cytometry.

Circle = median GFP fluorescence value from one transfection, 10,000 cells; bars = means of three transfections. In B and C, asterisks (*) = $p < 0.05$ for experimental mean compared to the NA control mean.

DISCUSSION

We have demonstrated that DNA enhancer elements and fusion proteins derived from endogenous mammalian systems can be used to support strong expression from transgenes. Furthermore, we have successfully demonstrated long-term reactivation of a transgene that had been previously silenced by ectopic Polycomb heterochromatin. Transient induction of activation by Gal4-AAPs is sufficient to maintain an active state over nearly fifteen generations of cell division. These results have exciting implications for achieving reliable expression of synthetic DNA in engineered cells, as well as our understanding of inherited chromatin states.

Our results also suggest that the mechanism of artificial transgene reactivation within Polycomb heterochromatin requires assembly of transcription initiation complexes. From STRING analysis, we found no clear pattern of histone modifications to distinguish the inactive Gal4-AAPs from activators that were able to enhance expression in Polycomb heterochromatin (Fig. 1). We observed that several of the fusion proteins did not restore expression from the Polycomb-repressed *luciferase* transgene in HEK293 cells (Fig. 4a). Thus, Gal4-tethered proteins might be functional but not sufficient, are non-functional (sterically hindered), or require positioning within non-coding DNA such as enhancer elements. For instance, a p300 fusion has shown strong activation of *MyoD* and *Oct4* when positioned 5-20 kb upstream at an enhancer [29]. Future work could be done to systematically test the AAPs at endogenous enhancers.

Upon further investigation we determined that assembly of the MYB TAD with P300/CBP is critical for Gal4-MYB-mediated activation within Polycomb chromatin. Inhibition of p300 HAT activity via C646 did not disrupt Gal4-MYB function (Fig. 6b). Furthermore, the Gal4 fusion that included only the p300 HAT domain failed to activate Polycomb-repressed *Tk-luciferase* (Fig. 3, Fig. 4). Therefore the p300 catalytic domain alone is neither necessary nor sufficient to reverse epigenetic silencing under the conditions tested here. CBP, which is also a histone acetyltransferase, might compensate for p300 in C646-treated cells [68]. Celastrol inhibits the interaction of p300/CBP with MYB by binding to the CBP KIX domain [69–72], and completely reduces Gal4-MYB activity (Fig. 6b). In contrast to C646, celastrol may disrupt the recruitment of both HAT enzymes, p300 and CBP.

In contrast to Gal4-MYB, the Gal4-p65 and -VP64 fusions showed robust activation of PRC-silenced luciferase in the presence of both inhibitors (Fig. 6b). Although VP64 (VP16) and p65 are known to interact with p300/CBP, they also interact with the large multi-subunit Mediator complex

to initiate transcription [77–79]. Multiple interactions of Gal4-p65 and -VP64 with Mediator may allow these proteins to function independently of p300/CBP [80]. However in the case of Gal4-MYB, cooperative interactions between p300/CBP and Mediator [81, 82] may be necessary for gene activation. In our study, Mediator complex recruitment arises as a particularly potent mechanism of transgene reactivation in Polycomb heterochromatin [82]. Mediator is known to cooperatively regulate PRC2 repression [83] and certain Mediator subunits are directly involved in the removal of PRC2 from endogenous promoters [84]. Similarly, Mediator has an antagonistic relationship with the PRC1 repression complex [85].

The inhibitor experiments also suggest a novel technique for chemically-inducible gene regulation in mammalian cells. The ability to quickly toggle between enhanced and repressed states is a cornerstone technology for the control of engineered transgenic systems [26, 86, 87]. Current methods for toggling gene expression in mammalian cells employ drug-mediated transactivator localization, such as allosteric modulation of DNA-binding protein domains [26, 86, 88], blue light-responsive CRY proteins [89], and chemically induced dimerization (CID) systems [90–92], or RNA interference to deplete the regulator [87]. To our knowledge, no systems currently exist where the transactivation module's activity (i.e., MYB-CBP binding) is modulated by a small molecule drug. Celastrol has a low toxicity and is in fact being explored as a therapeutic due to its positive effects on the immune system [93–95]. The concentration of celastrol that is sufficient to toggle Gal4-MYB activity in polycomb chromatin is well below any reported LD50 values for celastrol [96–100].

Finally, our work demonstrates the potential flexibility of MYB fusion proteins as transactivators. dCas9-MYB showed strong activation of previously silenced transgenes near two different promoter elements, *Tk* and *CMV*. *Tk* had undergone silencing by ectopic polycomb chromatin, whereas *CMV* had become silenced by undetermined mechanisms. Interestingly, stimulation of expression from PRC-repressed *Tk* seemed to require TSS-proximal positioning of Gal4-MYB , whereas Gal4-MYB stimulated expression from both upstream (up to 1400 bp) and downstream (up to 350 bp) of the CMV TSS. Factors that might account for this difference include intrinsic differences in the core promoter sequences, the presence of cryptic enhancers at one promoter and not the other, and differences in chromatin structure. To our knowledge, our work represents the first use of MYB as a dCas9 fusion that can activate a transgene from proximal and distal locations.

CONCLUSION

In conclusion, we have determined a predominant role for p300/CBP-recruiting transcriptional activators in the reversal of Polycomb-mediated expression in the context of synthetic transgene

regulation. In particular, we have expanded the characterization of the transcriptional activator protein MYB and its associated enhancer DNA sequence for applications in artificial gene regulation in mammalian cells.

METHODS

Construction and Testing of Plasmids containing MYB- and p65 Motifs

Plasmid construction, transfection of PC-3 cells, and luciferase assays were carried out as described previously [12]. Briefly, cloning of double-stranded oligos was used to insert motifs 222 bp upstream of the transcription start site of an EF1a promoter at XbaI/SphI. Plasmids were then transfected into PC-3 cells (ATCC, CRL-1435) using Lipofectamine LTX™ following the manufacturer's recommended protocols. Luciferase expression was measured 48 hours after transfection using a luciferase assay kit (Promega, Madison, WI). All luciferase values were normalized relative to the native plasmid control, which contained an unaltered EF1a promoter.

Construction of MV14 and Gal4-AAP Plasmids

We constructed mammalian expression vector 14 (MV14) for the overexpression of Gal4-mCherry-AAP fusion proteins in-frame with a nuclear localization sequence and 6X-histidine tag. First, plasmid MV13 was built by inserting a Gal4-mCherry fragment into MV10 [101] directly downstream of the CMV promoter. Next, MV14 was built by inserting a SpeI/PstII (FastDigest enzymes, ThermoFisher Scientific) -digested gBlock Gene Fragment (Integrated DNA Technologies), which encoded a XbaI/NotI multiple cloning site, into MV13 downstream of mCherry. Ligation reactions included gel-purified (Sigma NA1111) DNA (25 ng linearized vector, a 2x molar ratio of insert fragments), 1x Roche RaPID ligation buffer, 1.0 uL T4 ligase (New England Biolabs), in a final volume of 10uL.

AAPs were cloned into MV14 at the multiple cloning site containing XbaI and NotI cut sites. AAPs were either ordered from DNASU in vectors and amplified using primers that added a 5' XbaI site and a 3' NotI site or ordered as gBlock Gene Fragments with the same 5' and 3' cutsites (Integrated DNA Technologies). Sequences in vectors were amplified with Phusion High Fidelity DNA Polymerase (New England BioLabs) and primers listed in Supplemental Table S2. MV14 and AAP inserts were double-digested with FastDigest *XbaI* and FastDigest *NotI* (ThermoFisher Scientific) and then ligated with T4 DNA ligase (New England Biolabs). MV14_AAP plasmids are publically available through DNASU (Supplemental Table S4)

Cell Culturing and Transfections

Luc14 and Gal4-EED/luc HEK293 cells were grown in Gibco DMEM high glucose 1× (Life Technologies) with 10% Tet-free Fetal Bovine Serum (FBS) (Omega Scientific), 1% penicillin streptomycin (ATCC) at 37 °C in a humidified 5% CO_2 incubator. Gal4-EED/luc cells were treated with 1 µg/mL doxycycline (Santa Cruz Biotechnology) for 2 days to induce stable polycomb repression. Dox was removed and cells were cultured for another four days before being seeded in 12-well plates. Luc14 cells and dox-induced Gal4-EED/luc cells were seeded in 12-well plates such that cells reached 90% confluency for lipid-mediated transfection. Transfections were performed with 1 µg plasmid per well, 3 µL Lipofectamine LTX, and 1 µL Plus Reagent (Life Technologies) per the manufacturer's protocol. Seventy-two hours post transfection, cells were either collected for analysis or passaged further.

Puromycin selection was carried out on Gal4-AAP-expressing cells for the experiments represented in Figure 5 and Supplemental Figure S1. Dox-treated Gal4-EED/luc cells were transfected in 12-well plates and then grown for 24 hours before the addition of 10 µg/mL puromycin (Santa Cruz Biotechnology) to Gibco DMEM high glucose 1× (Life Technologies) with 10% Tet-free Fetal Bovine Serum (FBS) (Omega Scientific), 1% penicillin streptomycin (ATCC). Cells were grown in puromycin containing media for two days before wash out.

Luciferase Assays

Luciferase assays were performed as previously described in Tekel *et al.* [101]. In brief, a single well of cells from a 12 well tissue culture plate was collected per independent transfection in 1.5mL 1X PBS. Cells were loaded into 9 wells of a Black Costar Clear Bottom 96 Well Plates (Corning #3631). Three wells of cells were used to detect mCherry in order to quantify Gal4-AAP proteins. A 2X Hoechst 33342 stain (Invitrogen #H3570) was loaded into three more wells to stain nuclear DNA in order to quantify cell density. The final three wells were prepared with Luciferase Assay Buffer (Biotium #30085). Plates were scanned in a microplate reader (Biotek Synergy H1) to detect RFP (580 nm - 610 nm), Hoechst 33342 fluorescence (360 nm - 460 nm) and chemiluminescence from the same sample in parallel.

RT-qPCR

We prepared total RNA from ~1.0 x 10^6 cells (Qiagen RNeasy Mini kit 74104) and generated cDNA from 2 µg of total RNA and the SuperScript III First Strand Synthesis system (Invitrogen #18080051) in a reaction volume of 20 µl. Quantitative PCR (qPCR) was performed with universal primers against the mCherry portion of the Gal4-AAP fusions, or the *TATA binding protein* (*TBP*) housekeeping gene. Triplicate qPCR reactions (10 µl) each contained SYBR Green 1 2X master mix (Roche), 2 µl of a 1:10 cDNA dilution, and 750 nM of each primer (forward and reverse, see

Supplemental Table S5). We calculated Mean Quantification Cycle (C_q) for three replicate wells per unique reaction. Change in gene expression level was calculated as $\Delta C_q = 2^{[\text{Mean Cp reference} - \text{Mean Cp target}]}$. Log2 fold change in gene expression was calculated as = $\log2(\Delta C_{q\ \text{transfected cells}} / \Delta C_{q\ \text{mock}})$.

Flow Cytometry

Cells were passed through a 35 µm nylon strainer (EMS #64750-25). Green fluorescent signal from GFP and red fluorescent signal from mCherry were detected on a BD Accuri C6 flow cytometer (675 nm LP filter) using CFlow Plus software. Data were further analyzed using FlowJo 10.5.3. One run (~10□000 live cells, gated by forward and side scatter) was completed per sample, allowing us to determine median fluorescence within the live cell population.

Construction of dCas9-MYB and Design of sgRNAs

We modified the vector pX330A_dCas9–1 × 4 (a gift from Takashi Yamamoto, Addgene plasmid #63598) by inserting a gBlock Gene Fragment (Integrated DNA Technologies) encoding the MYB TAD followed by a p2A signal [102] and *mCherry* after the *dCas9* ORF. The resulting vector expresses a dCas9-MYB fusion and mCherry as separate peptides from a single mRNA transcript. The vector and gBlock were digested with *FseI* (New England BioLabs) and FastDigest *Eco*RI (ThermoFisher Scientific) and ligated using T4 DNA Ligase (New England BioLabs). We named this new vector pX330g_dCas9-MYB. SgRNAs used in the study (Supplemental Table S3) were designed using the CRISPR design tool at crispr.mit.edu. DNA oligos were synthesized with BbsI overhangs for cloning into pX330g_dCas9-MYB (Integrative DNA Technology). Drop-in of sgRNAs followed the cloning protocol described in Cong *et al*. [103].

Celastrol and C646 Treatments

Gal4-EED/luc cells were induced with dox and transfected as described above. Three days post transfection, cells were treated with either C646 (Selleck Chemicals) or Celastrol (Selleck Chemicals) diluted to a concentration of 5µM in Gibco DMEM high glucose 1× (Life Technologies) with 10% Tet-free Fetal Bovine Serum (FBS) (Omega Scientific). Cells were incubated with the drug for six hours before being washed and either harvested for a luciferase assay or grown further in drug-free media.

Statistical Analyses

The differences of means were calculated using the two sample, one-tailed Student's *t* test. For $p < 0.05$, confidence was 95% for 2 degrees of freedom and a test statistic of $t_{(0.05,2)} = 2.920$. To evaluate significance of Gal4-MYB induced activation after the removal of celastrol and its subsequent re-addition, a nest one-way ANOVA was used with 95% confidence and two degrees of freedom.

LIST OF ABBREVIATIONS

AAP- activation associated peptide
CMV- cytomegalovirus
CR- chromatin remodeler
Gal4- Gal4 DNA binding domain
HAT- histone acetyltransferase
NLS- nuclear localization signal
ORF- open reading frame
PF- pioneer factor
PolII- RNA polymerase II
PRC- Polycomb repressive complex
TAD- transcriptional activation domain
UAS- upstream activation sequence

DECLARATIONS

Acknowledgements: The authors thank C. Liu and T. Loveless for generously providing cells with a silenced CMV-GFP transgene, K. Rege and R. Niti for celastrol and C646, and R. Daer and D. Vargas for early efforts on this work.

Availability of data and material: Sequences of plasmids used in this study are publically available as listed in Supplemental Table S4 as well as physically available in the DNASU plasmid repository.

Competing interests: The authors declare no competing interest.

Funding: This project was supported by NSF CBET grant 1403214. KAH was supported by National Institutes of Health NCI grant K01 CA188164.

Authors' contributions: CMB completed all Gal4- and dCas9-fusion cloning, HEK293 cell culture, luciferase assays, flow cytometry, and PCR related to targeted fusion activators. CMB also carried out experimental design, STRING analysis, statistical analyses, and manuscript writing. JE designed and performed PC-3 transfections with enhancer motif-EF1a-luciferase constructs, and luciferase assays. RM cloned the enhancer motif-EF1a-luciferase constructs. KAH oversaw all work, finalized graphics for the figures, and assisted with manuscript preparation and submission. All authors reviewed and approved the manuscript.

Ethics approval and consent to participate: Not applicable to this work.

Consent for publication: Not applicable to this work.

REFERENCES

1. Brooks AR, Harkins RN, Wang P, Qian HS, Liu P, Rubanyi GM. Transcriptional silencing is associated with extensive methylation of the CMV promoter following adenoviral gene delivery to muscle. J Gene Med. 2004;6:395–404.

2. Suzuki M, Cerullo V, Bertin TK, Cela R, Clarke C, Guenther M, et al. MyD88-dependent silencing of transgene expression during the innate and adaptive immune response to helper-dependent adenovirus. Hum Gene Ther. 2010;21:325–36.

3. Leung DC, Lorincz MC. Silencing of endogenous retroviruses: when and why do histone marks predominate? Trends Biochem Sci. 2012;37:127–33.

4. Ross PJ, Kennedy MA, Parks RJ. Host cell detection of noncoding stuffer DNA contained in helper-dependent adenovirus vectors leads to epigenetic repression of transgene expression. J Virol. 2009;83:8409–17.

5. Ellis J. Silencing and variegation of gammaretrovirus and lentivirus vectors. Hum Gene Ther. 2005;16:1241–6.

6. Gong L, Liu F, Xiong Z, Qi R, Luo Z, Gong X, et al. Heterochromatin protects retinal pigment epithelium cells from oxidative damage by silencing p53 target genes. Proc Natl Acad Sci U S A. 2018;115:E3987–95.

7. Erhardt S, Lyko F, Ainscough JF-X, Surani MA, Paro R. Polycomb-group proteins are involved in silencing processes caused by a transgenic element from the murine imprinted H19/Igf2 region in Drosophila. Dev Genes Evol. 2003;213:336–44.

8. Dufourt J, Brasset E, Desset S, Pouchin P, Vaury C. Polycomb group-dependent, heterochromatin protein 1-independent, chromatin structures silence retrotransposons in somatic tissues outside ovaries. DNA Res. 2011;18:451–61.

9. Otte AP, Kwaks THJ. Gene repression by Polycomb group protein complexes: a distinct complex for every occasion? Curr Opin Genet Dev. 2003;13:448–54.

10. Johansen J, Tornøe J, Møller A, Johansen TE. Increased in vitro and in vivo transgene

expression levels mediated through cis-acting elements. J Gene Med. 2003;5:1080–9.

11. Cheng JK, Alper HS. Transcriptomics-Guided Design of Synthetic Promoters for a Mammalian System. ACS Synth Biol. 2016;5:1455–65.

12. Zimmerman D, Patel K, Hall M, Elmer J. Enhancement of transgene expression by nuclear transcription factor Y and CCCTC-binding factor. Biotechnol Prog. 2018. doi:10.1002/btpr.2712.

13. Wang W, Guo X, Li Y-M, Wang X-Y, Yang X-J, Wang Y-F, et al. Enhanced transgene expression using cis-acting elements combined with the EF1 promoter in a mammalian expression system. Eur J Pharm Sci. 2018;123:539–45.

14. Roberts ML, Katsoupi P, Tseveleki V, Taoufik E. Bioinformatically Informed Design of Synthetic Mammalian Promoters. Methods Mol Biol. 2017;1651:93–112.

15. Saxena P, Bojar D, Fussenegger M. Design of Synthetic Promoters for Gene Circuits in Mammalian Cells. In: Methods in Molecular Biology. 2017. p. 263–73.

16. Chavez A, Scheiman J, Vora S, Pruitt BW, Tuttle M, Iyer E, et al. Highly-efficient Cas9-mediated transcriptional programming. 2014. doi:10.1101/012880.

17. Konermann S, Brigham MD, Trevino AE, Joung J, Abudayyeh OO, Barcena C, et al. Genome-scale transcriptional activation by an engineered CRISPR-Cas9 complex. Nature. 2015;517:583–8.

18. Huang Y-H, Su J, Lei Y, Brunetti L, Gundry MC, Zhang X, et al. DNA epigenome editing using CRISPR-Cas SunTag-directed DNMT3A. Genome Biol. 2017;18:176.

19. Black JB, Adler AF, Wang H-G, D'Ippolito AM, Hutchinson HA, Reddy TE, et al. Targeted Epigenetic Remodeling of Endogenous Loci by CRISPR/Cas9-Based Transcriptional Activators Directly Converts Fibroblasts to Neuronal Cells. Cell Stem Cell. 2016;19:406–14.

20. Gao X, Tsang JCH, Gaba F, Wu D, Lu L, Liu P. Comparison of TALE designer transcription factors and the CRISPR/dCas9 in regulation of gene expression by targeting enhancers. Nucleic Acids Res. 2014;42:e155.

21. Zhang Y, Yin C, Zhang T, Li F, Yang W, Kaminski R, et al. CRISPR/gRNA-directed synergistic activation mediator (SAM) induces specific, persistent and robust reactivation of the HIV-1 latent reservoirs. Sci Rep. 2015;5:16277.

22. Daer RM, Cutts JP, Brafman DA, Haynes KA. The Impact of Chromatin Dynamics on Cas9-Mediated Genome Editing in Human Cells. ACS Synth Biol. 2017;6:428–38.

23. Clapier CR, Iwasa J, Cairns BR, Peterson CL. Mechanisms of action and regulation of ATP-dependent chromatin-remodelling complexes. Nat Rev Mol Cell Biol. 2017;18:407–22.

24. Zaret KS, Carroll JS. Pioneer transcription factors: establishing competence for gene expression. Genes Dev. 2011;25:2227–41.

25. Magnani L, Eeckhoute J, Lupien M. Pioneer factors: directing transcriptional regulators within the chromatin environment. Trends Genet. 2011;27:465–74.

26. Kramer BP, Viretta AU, Daoud-El-Baba M, Aubel D, Weber W, Fussenegger M. An engineered epigenetic transgene switch in mammalian cells. Nat Biotechnol. 2004;22:867–70.

27. Kwaks THJ, Sewalt RGAB, van Blokland R, Siersma TJ, Kasiem M, Kelder A, et al. Targeting of a histone acetyltransferase domain to a promoter enhances protein expression levels in mammalian cells. J Biotechnol. 2005;115:35–46.

28. Santillan DA, Theisler CM, Ryan AS, Popovic R, Stuart T, Zhou M-M, et al. Bromodomain and histone acetyltransferase domain specificities control mixed lineage leukemia phenotype. Cancer Res. 2006;66:10032–9.

29. Hilton IB, D'Ippolito AM, Vockley CM, Thakore PI, Crawford GE, Reddy TE, et al. Epigenome editing by a CRISPR-Cas9-based acetyltransferase activates genes from promoters and enhancers. Nat Biotechnol. 2015;33:510–7.

30. Cano-Rodriguez D, Gjaltema RAF, Jilderda LJ, Jellema P, Dokter-Fokkens J, Ruiters MHJ, et al. Writing of H3K4Me3 overcomes epigenetic silencing in a sustained but context-dependent manner. Nat Commun. 2016;7. doi:10.1038/ncomms12284.

31. McGinty RK, Kim J, Chatterjee C, Roeder RG, Muir TW. Chemically ubiquitylated histone H2B stimulates hDot1L-mediated intranucleosomal methylation. Nature. 2008;453:812–6.

32. O'Geen H, Ren C, Nicolet CM, Perez AA, Halmai J, Le VM, et al. dCas9-based epigenome editing suggests acquisition of histone methylation is not sufficient for target gene repression. Nucleic Acids Res. 2017;45:9901–16.

33. Aloia L, Di Stefano B, Di Croce L. Polycomb complexes in stem cells and embryonic development. Development. 2013;140:2525–34.

34. Poynter ST, Kadoch C. Polycomb and trithorax opposition in development and disease. Wiley Interdiscip Rev Dev Biol. 2016;5:659–88.

35. Schuettengruber B, Bourbon H-M, Di Croce L, Cavalli G. Genome Regulation by Polycomb and Trithorax: 70 Years and Counting. Cell. 2017;171:34–57.

36. Simon JA, Kingston RE. Occupying chromatin: Polycomb mechanisms for getting to genomic targets, stopping transcriptional traffic, and staying put. Mol Cell. 2013;49:808–24.

37. Beerli RR, Segal DJ, Dreier B, Barbas CF 3rd. Toward controlling gene expression at will: specific regulation of the erbB-2/HER-2 promoter by using polydactyl zinc finger proteins constructed from modular building blocks. Proc Natl Acad Sci U S A. 1998;95:14628–33.

38. Liu PQ, Rebar EJ, Zhang L, Liu Q, Jamieson AC, Liang Y, et al. Regulation of an endogenous locus using a panel of designed zinc finger proteins targeted to accessible chromatin regions. Activation of vascular endothelial growth factor A. J Biol Chem. 2001;276:11323–34.

39. Weston K, Michael Bishop J. Transcriptional activation by the v-myb oncogene and its cellular progenitor, c-myb. Cell. 1989;58:85–93.

40. Vo N, Goodman RH. CREB-binding Protein and p300 in Transcriptional Regulation. J Biol Chem. 2001;276:13505–8.

41. Zhao Q, Rank G, Tan YT, Li H, Moritz RL, Simpson RJ, et al. PRMT5-mediated methylation of histone H4R3 recruits DNMT3A, coupling histone and DNA methylation in gene silencing. Nat Struct Mol Biol. 2009;16:304–11.

42. Antonysamy S, Bonday Z, Campbell RM, Doyle B, Druzina Z, Gheyi T, et al. Crystal structure

of the human PRMT5:MEP50 complex. Proc Natl Acad Sci U S A. 2012;109:17960–5.

43. Alver BH, Kim KH, Lu P, Wang X, Manchester HE, Wang W, et al. The SWI/SNF chromatin remodelling complex is required for maintenance of lineage specific enhancers. Nat Commun. 2017;8:14648.

44. Clark KL, Halay ED, Lai E, Burley SK. Co-crystal structure of the HNF-3/fork head DNA-recognition motif resembles histone H5. Nature. 1993;364:412–20.

45. Kadoch C, Williams RT, Calarco JP, Miller EL, Weber CM, Braun SMG, et al. Dynamics of BAF-Polycomb complex opposition on heterochromatin in normal and oncogenic states. Nat Genet. 2017;49:213–22.

46. Kia SK, Gorski MM, Giannakopoulos S, Verrijzer CP. SWI/SNF mediates polycomb eviction and epigenetic reprogramming of the INK4b-ARF-INK4a locus. Mol Cell Biol. 2008;28:3457–64.

47. Lau PNI, Cheung P. Histone code pathway involving H3 S28 phosphorylation and K27 acetylation activates transcription and antagonizes polycomb silencing. Proc Natl Acad Sci U S A. 2011;108:2801–6.

48. Gehani SS, Agrawal-Singh S, Dietrich N, Christophersen NS, Helin K, Hansen K. Polycomb group protein displacement and gene activation through MSK-dependent H3K27me3S28 phosphorylation. Mol Cell. 2010;39:886–900.

49. Josefowicz SZ, Shimada M, Armache A, Li CH, Miller RM, Lin S, et al. Chromatin Kinases Act on Transcription Factors and Histone Tails in Regulation of Inducible Transcription. Mol Cell. 2016;64:347–61.

50. Tie F, Banerjee R, Stratton CA, Prasad-Sinha J, Stepanik V, Zlobin A, et al. CBP-mediated acetylation of histone H3 lysine 27 antagonizes Drosophila Polycomb silencing. Development. 2009;136:3131–41.

51. Englert NA, Luo G, Goldstein JA, Surapureddi S. Epigenetic Modification of Histone 3 Lysine 27. J Biol Chem. 2014;290:2264–78.

52. Christensen MD, Nitiyanandan R, Meraji S, Daer R, Godeshala S, Goklany S, et al. An inhibitor screen identifies histone-modifying enzymes as mediators of polymer-mediated transgene expression from plasmid DNA. J Control Release. 2018;286:210–23.

53. Gracey Maniar LE, Maniar JM, Chen Z-Y, Lu J, Fire AZ, Kay MA. Minicircle DNA vectors achieve sustained expression reflected by active chromatin and transcriptional level. Mol Ther. 2013;21:131–8.

54. Riu E, Chen Z-Y, Xu H, He C-Y, Kay MA. Histone modifications are associated with the persistence or silencing of vector-mediated transgene expression in vivo. Mol Ther. 2007;15:1348–55.

55. Mathelier A, Fornes O, Arenillas DJ, Chen C-Y, Denay G, Lee J, et al. JASPAR 2016: a major expansion and update of the open-access database of transcription factor binding profiles. Nucleic Acids Res. 2016;44:D110–5.

56. Zobel A, Kalkbrenner F, Vorbrueggen G, Moelling K. Transactivation of the human c-myc gene by c-Myb. Biochem Biophys Res Commun. 1992;186:715–22.

57. Kawasaki H, Schiltz L, Chiu R, Itakura K, Taira K, Nakatani Y, et al. ATF-2 has intrinsic histone acetyltransferase activity which is modulated by phosphorylation. Nature. 2000;405:195–200.

58. Yang L, Wang H, Luo X, Mao P, Tian W, Shi Y, et al. Virion protein 16 induces demethylation of DNA integrated within chromatin in a novel mammalian cell model. Acta Biochim Biophys Sin . 2011;44:154–61.

59. Milne TA, Briggs SD, Brock HW, Martin ME, Gibbs D, Allis CD, et al. MLL targets SET domain methyltransferase activity to Hox gene promoters. Mol Cell. 2002;10:1107–17.

60. Nishioka K, Chuikov S, Sarma K, Erdjument-Bromage H, Allis CD, Tempst P, et al. Set9, a novel histone H3 methyltransferase that facilitates transcription by precluding histone tail modifications required for heterochromatin formation. Genes Dev. 2002;16:479–89.

61. Serandour AA, Avner S, Percevault F, Demay F, Bizot M, Lucchetti-Miganeh C, et al. Epigenetic switch involved in activation of pioneer factor FOXA1-dependent enhancers. Genome Res. 2011;21:555–65.

62. Wang W, Côté J, Xue Y, Zhou S, Khavari PA, Biggar SR, et al. Purification and biochemical heterogeneity of the mammalian SWI-SNF complex. EMBO J. 1996;15:5370–82.

63. Hansen KH, Bracken AP, Pasini D, Dietrich N, Gehani SS, Monrad A, et al. A model for transmission of the H3K27me3 epigenetic mark. Nat Cell Biol. 2008;10:1291–300.

64. Pirrotta V. Introduction to Polycomb Group Mechanisms. In: Polycomb Group Proteins. 2017. p. 1–3.

65. Sandberg ML, Sutton SE, Pletcher MT, Wiltshire T, Tarantino LM, Hogenesch JB, et al. c-Myb and p300 regulate hematopoietic stem cell proliferation and differentiation. Dev Cell. 2005;8:153–66.

66. Pattabiraman DR, Sun J, Dowhan DH, Ishii S, Gonda TJ. Mutations in multiple domains of c-Myb disrupt interaction with CBP/p300 and abrogate myeloid transforming ability. Mol Cancer Res. 2009;7:1477–86.

67. Raisner R, Kharbanda S, Jin L, Jeng E, Chan E, Merchant M, et al. Enhancer Activity Requires CBP/P300 Bromodomain-Dependent Histone H3K27 Acetylation. Cell Rep. 2018;24:1722–9.

68. Ogryzko VV, Louis Schiltz R, Russanova V, Howard BH, Nakatani Y. The Transcriptional Coactivators p300 and CBP Are Histone Acetyltransferases. Cell. 1996;87:953–9.

69. Coulibaly A, Haas A, Steinmann S, Jakobs A, Schmidt TJ, Klempnauer K-H. The natural anti-tumor compound Celastrol targets a Myb-C/EBPβ-p300 transcriptional module implicated in myeloid gene expression. PLoS One. 2018;13:e0190934.

70. Uttarkar S, Piontek T, Dukare S, Schomburg C, Schlenke P, Berdel WE, et al. Small-Molecule Disruption of the Myb/p300 Cooperation Targets Acute Myeloid Leukemia Cells. Mol Cancer Ther. 2016;15:2905–15.

71. Denis CM, Langelaan DN, Kirlin AC, Chitayat S, Munro K, Spencer HL, et al. Functional redundancy between the transcriptional activation domains of E2A is mediated by binding to the KIX domain of CBP/p300. Nucleic Acids Res. 2014;42:7370–82.

72. Uttarkar S, Dassé E, Coulibaly A, Steinmann S, Jakobs A, Schomburg C, et al. Targeting acute

myeloid leukemia with a small molecule inhibitor of the Myb/p300 interaction. Blood. 2016;127:1173–82.

73. Wang Y-M, Gu M-L, Meng F-S, Jiao W-R, Zhou X-X, Yao H-P, et al. Histone acetyltransferase p300/CBP inhibitor C646 blocks the survival and invasion pathways of gastric cancer cell lines. Int J Oncol. 2017;51:1860–8.

74. Oike T, Komachi M, Ogiwara H, Amornwichet N, Saitoh Y, Torikai K, et al. C646, a selective small molecule inhibitor of histone acetyltransferase p300, radiosensitizes lung cancer cells by enhancing mitotic catastrophe. Radiother Oncol. 2014;111:222–7.

75. Bowers EM, Yan G, Mukherjee C, Orry A, Wang L, Holbert MA, et al. Virtual ligand screening of the p300/CBP histone acetyltransferase: identification of a selective small molecule inhibitor. Chem Biol. 2010;17:471–82.

76. Tsai SQ, Zheng Z, Nguyen NT, Liebers M, Topkar VV, Thapar V, et al. GUIDE-seq enables genome-wide profiling of off-target cleavage by CRISPR-Cas nucleases. Nat Biotechnol. 2015;33:187–97.

77. van Essen D, Engist B, Natoli G, Saccani S. Two Modes of Transcriptional Activation at Native Promoters by NF-κB p65. PLoS Biol. 2009;7:e1000073.

78. Thakore PI, Black JB, Hilton IB, Gersbach CA. Editing the epigenome: technologies for programmable transcription and epigenetic modulation. Nat Methods. 2016;13:127–37.

79. Wang W, Qin J-J, Voruganti S, Nag S, Zhou J, Zhang R. Polycomb Group (PcG) Proteins and Human Cancers: Multifaceted Functions and Therapeutic Implications. Med Res Rev. 2015;35:1220–67.

80. Lecoq L, Raiola L, Chabot PR, Cyr N, Arseneault G, Legault P, et al. Structural characterization of interactions between transactivation domain 1 of the p65 subunit of NF-κB and transcription regulatory factors. Nucleic Acids Res. 2017;45:5564–76.

81. Huang Z-Q, Li J, Sachs LM, Cole PA, Wong J. A role for cofactor-cofactor and cofactor-histone interactions in targeting p300, SWI/SNF and Mediator for transcription. EMBO J. 2003;22:2146–55.

82. Haas M, Siegert M, Schürmann A, Sodeik B, Wolfes H. c-Myb protein interacts with Rcd-1, a component of the CCR4 transcription mediator complex. Biochemistry. 2004;43:8152–9.

83. Fukasawa R, Iida S, Tsutsui T, Hirose Y, Ohkuma Y. Mediator complex cooperatively regulates transcription of retinoic acid target genes with Polycomb Repressive Complex 2 during neuronal differentiation. J Biochem. 2015;158:373–84.

84. Englert NA, Luo G, Goldstein JA, Surapureddi S. Epigenetic modification of histone 3 lysine 27: mediator subunit MED25 is required for the dissociation of polycomb repressive complex 2 from the promoter of cytochrome P450 2C9. J Biol Chem. 2015;290:2264–78.

85. Lehmann L, Ferrari R, Vashisht AA, Wohlschlegel JA, Kurdistani SK, Carey M. Polycomb repressive complex 1 (PRC1) disassembles RNA polymerase II preinitiation complexes. J Biol Chem. 2012;287:35784–94.

86. Oakes BL, Nadler DC, Flamholz A, Fellmann C, Staahl BT, Doudna JA, et al. Profiling of engineering hotspots identifies an allosteric CRISPR-Cas9 switch. Nat Biotechnol. 2016;34:646–51.

87. Greber D, El-Baba MD, Fussenegger M. Intronically encoded siRNAs improve dynamic range of mammalian gene regulation systems and toggle switch. Nucleic Acids Res. 2008;36:e101–e101.

88. Stanton BC, Siciliano V, Ghodasara A, Wroblewska L, Clancy K, Trefzer AC, et al. Systematic transfer of prokaryotic sensors and circuits to mammalian cells. ACS Synth Biol. 2014;3:880–91.

89. Mansouri M, Strittmatter T, Fussenegger M. Light-Controlled Mammalian Cells and Their Therapeutic Applications in Synthetic Biology. Adv Sci Lett. 2018;:1800952.

90. Inobe T, Nukina N. Rapamycin-induced oligomer formation system of FRB-FKBP fusion proteins. J Biosci Bioeng. 2016;122:40–6.

91. Rivera VM, Clackson T, Natesan S, Pollock R, Amara JF, Keenan T, et al. A humanized system for pharmacologic control of gene expression. Nat Med. 1996;2:1028–32.

92. DeRose R, Miyamoto T, Inoue T. Manipulating signaling at will: chemically-inducible dimerization (CID) techniques resolve problems in cell biology. Pflugers Arch. 2013;465:409–17.

93. Cascão R, Fonseca JE, Moita LF. Celastrol: A Spectrum of Treatment Opportunities in Chronic Diseases. Front Med. 2017;4:69.

94. Venkatesha SH, Dudics S, Astry B, Moudgil KD. Control of autoimmune inflammation by celastrol, a natural triterpenoid. Pathog Dis. 2016;74. doi:10.1093/femspd/ftw059.

95. Ju SM, Youn GS, Cho YS, Choi SY, Park J. Celastrol ameliorates cytokine toxicity and pro-inflammatory immune responses by suppressing NF-κB activation in RINm5F beta cells. BMB Rep. 2015;48:172–7.

96. Li G, Liu D, Zhang Y, Qian Y, Zhang H, Guo S, et al. Celastrol inhibits lipopolysaccharide-stimulated rheumatoid fibroblast-like synoviocyte invasion through suppression of TLR4/NF-κB-mediated matrix metalloproteinase-9 expression. PLoS One. 2013;8:e68905.

97. Raja SM, Clubb RJ, Ortega-Cava C, Williams SH, Bailey TA, Duan L, et al. Anticancer activity of Celastrol in combination with ErbB2-targeted therapeutics for treatment of ErbB2-overexpressing breast cancers. Cancer Biol Ther. 2011;11:263–76.

98. Yang H, Chen D, Cui QC, Yuan X, Dou QP. Celastrol, a triterpene extracted from the Chinese “Thunder of God Vine,” is a potent proteasome inhibitor and suppresses human prostate cancer growth in nude mice. Cancer Res. 2006;66:4758–65.

99. Cleren C, Calingasan NY, Chen J, Beal MF. Celastrol protects against MPTP- and 3-nitropropionic acid-induced neurotoxicity. J Neurochem. 2005;94:995–1004.

100. Konieczny J, Jantas D, Lenda T, Domin H, Czarnecka A, Kuter K, et al. Lack of neuroprotective effect of celastrol under conditions of proteasome inhibition by lactacystin in in vitro and in vivo studies: implications for Parkinson’s disease. Neurotox Res. 2014;26:255–73.

101. Tekel SJ, Barrett C, Vargas D, Haynes KA. Design, Construction, and Validation of Histone-Binding Effectors in Vitro and in Cells. Biochemistry. 2018;57:4707–16.

102. Liu Z, Chen O, Blake Joseph Wall J, Zheng M, Zhou Y, Wang L, et al. Systematic comparison of 2A peptides for cloning multi-genes in a polycistronic vector. Sci Rep. 2017;7. doi:10.1038/s41598-017-02460-2.

103. Cong L, Ran FA, Cox D, Lin S, Barretto R, Habib N, et al. Multiplex genome engineering using CRISPR/Cas systems. Science. 2013;339:819–23.